Conference materials
UDC 533
DOI: https://doi.org/10.18721/JPM.161.202

Radiative energy losses of a high-current vacuum arc with an eroding anode

K.K. Zabello [1]✉, Yu.A. Barinov [1], A.A. Logachev [1],
I.N. Poluyanova [2], E.V. Sherstnev [1], S.M. Shkol'nik [1]

[1] Ioffe Institute, St. Petersburg, Russia;
[2] Switchgear design bureau LTD, Sevastopol, Russia
✉ zabellok@mail.ioffe.ru

Abstract. The results of measurements of the radiation power of a vacuum ($p \sim 10^{-4}$ Pa) arc in the near infrared, visible and ultraviolet regions of the spectrum (200 nm $\leq \lambda \leq$ 1100 nm) are presented. The arc burned on industrial AMF-electrodes with a diameter of 55 mm. The material of the electrodes was the CuCr30 composition. The arc was fed by a current pulse in the shape close to half of the industrial frequency sine wave ($f = 50$Hz). The radiation was output through one of the side windows of the vacuum chamber. The window was made of quartz KU-1. The radiation receiver was a silicon photodiode with a diameter of 1.2 mm, located outside the vacuum chamber on an axis intersecting with the axis of symmetry of the discharge in the center of the interelectrode gap. The signal from the photodiode was taken through an amplifier and recorded on an oscilloscope. Considering the spectral sensitivity of the diode, two series of measurements were made: measurements without a filter and through a ZhS-10 yellow filter that cuts off radiation with $\lambda \leq 400$ nm. The results obtained made it possible to analyze the dependence of the radiation power on the arc current at different stages of its development. The results showed that at high currents in the developed vacuum arc with anodic activity (eroding anode), a significant part (up to 15%) of the power released in the arc is transferred by radiation.

Keywords: vacuum arc, axial magnetic field, radiation power

Citation: Zabello K.K., Barinov Yu.A., Logachev A.A., Poluyanova I.N., Sherstnev E.V., Shkol'nik S.M., Radiative energy losses of a high-current vacuum arc with an eroding anode, St. Petersburg State Polytechnical University Journal. Physics and Mathematics. 16 (1.2) (2023) 18–24. DOI: https://doi.org/10.18721/JPM.161.202

Материалы конференции
УДК 533
DOI: https://doi.org/10.18721/JPM.161.202

Излучательные потери энергии сильноточной вакуумной дуги с эродирующим анодом

К.К. Забелло [1]✉, Ю.А. Баринов [1], А.А. Логачёв [1],
И.Н. Полуянова [2], Е.В. Шерстнев [1], С.М. Школьник [1]

[1] Физико-технический институт им. А.Ф. Иоффе РАН, Санкт-Петербург, Россия;
[2] Конструкторское бюро коммутационной аппаратуры, г. Севастополь, Россия
✉ zabellok@mail.ioffe.ru

Аннотация. Приведены результаты измерений мощности излучения вакуумной ($p \sim 10^{-4}$ Па) дуги в ближней инфракрасной, видимой и ультрафиолетовой областях спектра (200 нм $\leq \lambda \leq$ 1100 нм). Дуга горела на индустриальных АМП-электродах диаметром 55 мм. Материал электродов – композиция CuCr30. Дуга питалась импульсом

тока по форме близким к половине синусоиды промышленной частоты (f = 50 Гц). Излучение выводилось через одно из боковых окон вакуумной камеры. Окно было изготовлено из кварца КУ-1. Приемником излучения являлся кремниевый фотодиод диаметром 1,2 мм, расположенный вне вакуумной камеры на оси, пересекающейся с осью симметрии разряда в центре межэлектродного промежутка. Сигнал с фотодиода снимался через усилитель и фиксировался на осциллографе. Учитывая вид спектральной чувствительности диода, сделаны две серии измерений: измерения без фильтра и через фильтр ЖС-10, отрезающий излучение с $\lambda \leq 400$ nm. Полученные результаты позволили проанализировать зависимость мощности излучения от тока дуги на разных стадиях ее развития. Результаты показали, что при больших плотностях тока в развившейся вакуумной дуге с анодной активностью (эродирующим анодом) значительная часть мощности переносится излучением.

Ключевые слова: вакуумная дуга, магнитное поле, мощность излучения

Ссылка при цитировании: Забелло К.К., Баринов Ю.А., Логачёв А.А., Полуянова И.Н., Шерстнёв Е.В., Школьник С.М. Излучательные потери энергии сильноточной вакуумной дуги с эродирующим анодом // Научно-технические ведомости СПбГПУ. Физико-математические науки. 2023. Т. 16. № 1.2. С. 18–24. DOI: https://doi.org/10.18721/JPM.161.202

Introduction

A great interest in the research of a high-current vacuum arc is connected not only with the fact that this type of electric discharge is still insufficiently studied, but also with the fact that the results of these studies are widely used. They are used in the creation of vacuum interrupters (VI), which are the main part of various vacuum switching devices. Therefore, high-current vacuum arcs burning under conditions characteristic of arc burning in the VI are intensively studied all over the world. One of the most important areas of work is the study of the energy balance of the arc at high currents.

It is known that in high-current high-pressure gas arcs, a significant part of the energy is transferred by radiation [1]. Radiation plays a more significant role in the energy balance of the arc, the greater the plasma density ($\sim n^2$). Unlike gas arcs, energy transfer by radiation in vacuum arcs has not been practically investigated. In mathematical modeling of vacuum arcs, radiation is most often not taken into account. There are only a few approximate calculations in which radiation was taken into account when considering the energy balance of the arc (for example, [2]). Experimental measurements of the radiation power from a high-current vacuum arc were not carried out before the start of this work.

Our first publication on this topic [3] presents the results obtained in a vacuum arc with artificial ignition, burning on end model electrodes in an external magnetic field. The arc radiation power was measured in the ultraviolet, as well as in the visible and near-infrared regions of the spectrum (200 nm $\leq \lambda \leq$ 1100 nm). This publication presents the results of measurements of radiation coming out of a vacuum arc burning on industrial electrodes generating their own axial magnetic field (such electrodes are called AMF-electrodes). The arc was ignited by opening the electrodes as it happens in the VI. Measurements were carried out in the same spectral intervals.

Materials and Methods

The experimental setup is described in detail in previous publications [4]. Here we will briefly indicate only the main parameters and make the necessary explanations. The experiments were carried out in a demountable vacuum chamber with continuous pumping ($p \sim 10^{-4}$ Pa). The camera had windows for photographing the arc and output radiation. The electrodes were positioned vertically. The upper electrode (anode) was stationary, and the lower (cathode) could move. In the initial state, the electrodes were closed and spring-loaded. The standard drive detached the lower electrode from the upper one, and it started moving at a mean speed of ~ 1 m/s. When the electrodes were opened, a vacuum arc appeared. The arc was powered by a current pulse having a shape close to half of the industrial frequency sine wave (f = 50 Hz). The opening of the electrodes occurred within the first

millisecond after the start of the current, so the duration of arc was 9–10 ms. The appearance of the electrodes is shown in Fig. 1. The same figure shows the radial distribution of the z-component of the magnetic field generated inside the interelectrode gap when the discharge current flows through the electrode system. The diameter of the electrode is 55 mm, the material of the working part of the electrode is the composition CuCr30. Erosion damage of the electrodes was controlled by periodically opening the vacuum chamber and photographing the working surface of the electrodes. Video recording of the arc was carried out through a side window using a Phantom MIRO M310 camera equipped with a Carl Zeiss 100/2 lens. In order not to overload the camera, dense neutral filters were used.

The window through which the analyzed radiation was output was made of quartz KU-1. The transmission of the window at $\lambda = 200$ nm was 60%. The dusting of the window was monitored and eliminated as needed. The arc radiation was recorded by a photodiode FDUC-1UST (JSC Technoexan). The photosensitive element of the diode had a diameter of $\mathbf{d} = 1.2$ mm. The signal from the photodiode was taken through a trans-impedance amplifier with a conversion factor of 1360 V/A, a bandwidth of 0–300 MHz. The diode was located outside the vacuum chamber on the x axis intersecting with the axis of symmetry of the discharge z in the center of the interelectrode gap. The distance from the z axis to the diode was 1350 mm. Such a large distance is chosen to avoid overloading the diode. The spectral sensitivity of the diode is shown in Fig. 2. Considering the spectral sensitivity of the diode, two series of measurements were made – measurements without a filter and through a ZhS-10 yellow filter that cuts off radiation with $\lambda \leq 400$ nm (Fig. 2). An oscilloscope was used to measure the signal from the diode. Other electrical signals were recorded on the same oscilloscope: the current and voltage of arc, as well as the signal from the sensor of the position of the electrodes. An Agilent DSO 5014A oscilloscope with a differential probe N2772A was used. All recordings from the oscilloscope were transferred to the computer. Before the measurements, the electrodes were cleaned by a series of kiloampere pulses. Fig. 3 shows an example of recording measurement results at close current values with and without the ZhS-10 filter. The maximum current amplitude in these experiments was 47 kA.

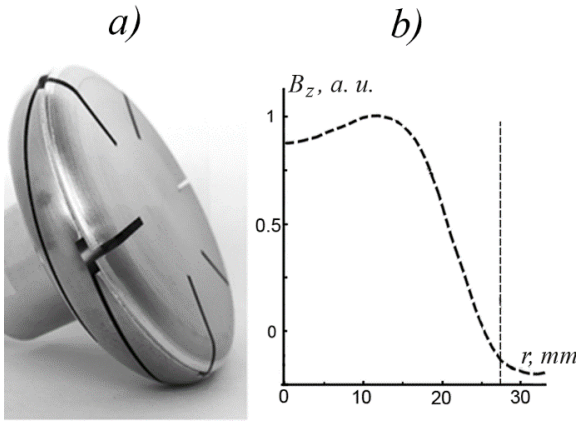

Fig. 1. Photo of the electrode (*a*), Radial distribution of the z-components of the magnetic field in the middle of the interelectrode gap (*b*)

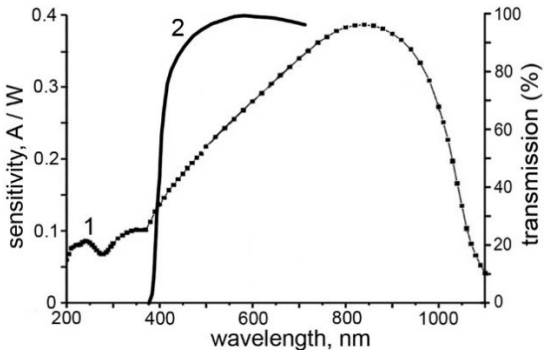

Fig. 2. Spectral sensitivity of the diode (1) and transmission of the ZhS-10 filter (2)

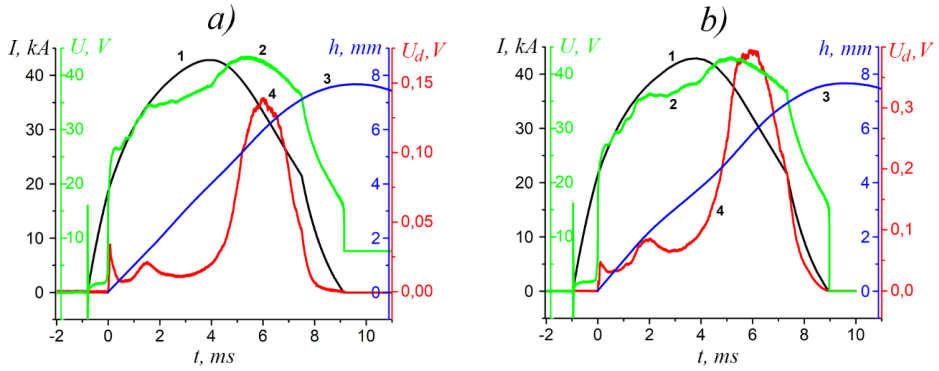

Fig. 3. Examples of recordings of experimental results at close currents when using a filter (*a*) and without a filter (*b*) for current (1), arc voltage (2), arc gap (3), and photodiode voltage (4)

Results and Discussion

Description of the discharge

The behavior of the arc on AMF electrodes under similar conditions was described in detail in previous articles [4, 5]. Therefore, here we will describe the arc briefly. Video shooting showed that the arc can be ignited at one point or at several points at once. Ignition at several points usually occurs if the opening of the electrodes began at a current of 8–10 kA or more. Immediately after ignition, the current density in the arc attachment is very high. After ignition, the cathode attachment of the arc increases in size and the current density in the attachment decreases. At some distance from it, new attachments appeared in different directions. The new attachments seem to jump on the surface and are fixed on the cuts of the electrode (see Fig. 1). As the attachment expands and the arc lengthens, the attachment structure and individual cathode spots become visible. The arc moves along the cathode and covers an increasing part of its surface. This process lasts 2–3 ms after ignition, after which the entire working surface of the cathode is covered by an arc. That is, the transition process is being completed.

The arc is symmetrized and centralized. This time corresponds to the penetration time of the AMF created by the electrodes when the arc current flows through them. Further, the arc burns steadily up to zero current. The arc voltage at the stage of its development and establishment (i.e., at the first milliseconds) depends not so much on the current as on the ignition conditions and with single-point ignition significantly exceeds the arc voltage with multipoint ignition. After the arc is established, the voltage is determined by the current (Fig. 4, *a*, curves 1, 2, 3). A gentle voltage maximum is reached approximately (0.5–1.0) ms after the current maximum, which is explained by the lengthening of the arc. This is how the voltage waveform looks at currents up to 32–34 kA. As the current increases, the shape of the waveform begins to change. After ≈ 3 ms after ignition, the voltage begins to grow faster. The maximum voltage becomes more pronounced and is reached after (1.5–2) ms after the maximum current (Fig. 4, *a*, curves 4. 5), or approximately 5.5–6 ms after ignition.

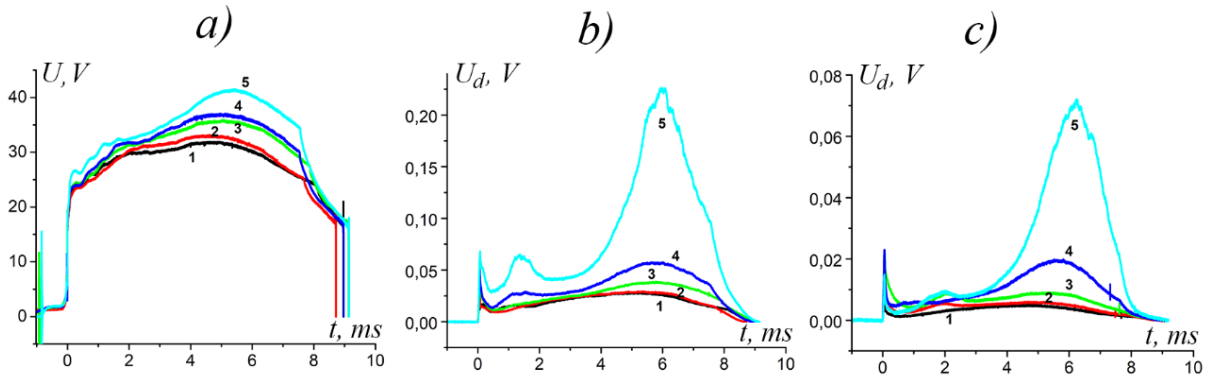

Fig. 4. Experimental time dependencies of arc voltage (*a*), the voltage of the diode without filter (*b*), the voltage of the diode with a filter (*c*) at the current of 24 (1), 28 (2), 32 (3), 37 (4), 41 (5) кА.

To construct the Current-Voltage characteristic (CVC), two characteristic time points were selected during the arc development: 3 ms after ignition, i.e. before the voltage begins to grow faster, and 5.5 ms after ignition, when the voltage reaches a maximum. As you can see, at currents less than 32–34 kA, both CVC are rectilinear. With an increase in the current, the CVC corresponding moment of 3 ms after ignition retains the slope, i.e. remains rectilinear. However, in the CVC corresponding to the time of 5.5 ms after ignition, a change occurs. Its slope increases, but the linearity remains (Fig. 5). A change (increase) in the slope of the CVC indicates that the properties of the arc plasma change, the arc resistance increases.

The signal from the photodiode shows the initial emission corresponding to the glow in sharply contracted cathode attachments. Further, at the initial stage of arc burning, the shape of the signal from the diode is determined by the development of the cathode attachment. In the developed arc, the signal from the diode is determined by the amplitude of the arc current (Fig. 4, *b*, curves 1, 2 ,3). This is typical for currents up to 32–34 kA. At higher currents, the signal from the diode after the arc is established begins to grow rapidly and reaches a maximum about 6 ms after ignition (Fig. 4, *b*, curves 4. 5).

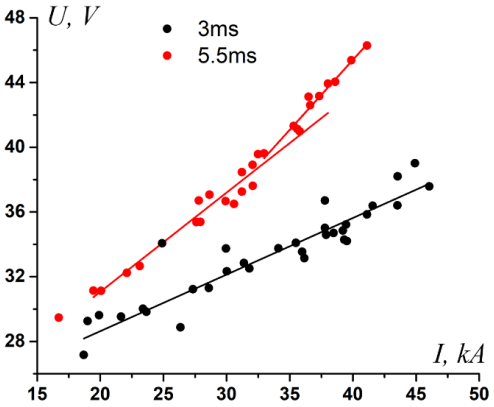

Fig. 5. Volt-ampere characteristics of the arc. The instantaneous values of the voltages and their corresponding currents are given for 3 and 5.5 ms after ignition

Photographing erosion traces on the surface of the electrodes showed that the anode is exposed to greater thermal effects than the cathode [6]. A light surface melt appears on the surface of the anode at moderate currents. At a current of approximately 32–34 kA, a significant part of the anode surface melts, traces of melt movement appear. When the current increases, the entire surface of the anode is melted, traces of intense melt movement are visible (Fig. 6). The dynamics of the melt is clearly visible on the video recordings of the arc and was described in detail in [4, 6], so here, due to the limited space, we will not delve into these issues. The cathode surface, as a whole, is fused weaker. Therefore, it clearly shows traces of deep melting, left by concentrated attachments, in the initial period of arc burning. The initial emissions noted above on the arc glow oscillogram are associated with the formation of the melt and evaporation from its surface.

As you can see (Fig. 4, 6), there are two modes of arc burning after the completion of its development and transition to a stable state. In the first mode, the arc does not glow as brightly as in the second. The thermal effect on the electrodes does not lead to their melting. In the second mode, the arc glows much stronger (by an order of magnitude or more), the electrodes, especially the anode, get very hot and melt, the arc resistance increases. The boundary between the modes passes in the area of current 32–34 kA for electrodes of this geometry. The modes differ in that in the second mode, the anode heats up so much that intense evaporation begins from its surface. The anode vapors entering the plasma are ionized, and the plasma concentration increases. With it, the radiation power increases as the square of the concentration. Such an arc mode is called a mode with anodic activity [5]. As can be seen from Fig. 4, the radiation power in the mode with anode activity increases greatly. Next, we will make estimates of the radiation power at different currents.

The power of radiation from the plasma.

In previous works [3, 7], the method of measurements and their processing is described in detail to determine the radiation power. Here we will only briefly recall the result. Using the ZhS-10 filter, we divide the radiation coming to the diode in the studied spectral region ($200 \leq \lambda \leq 1100$) nm into two

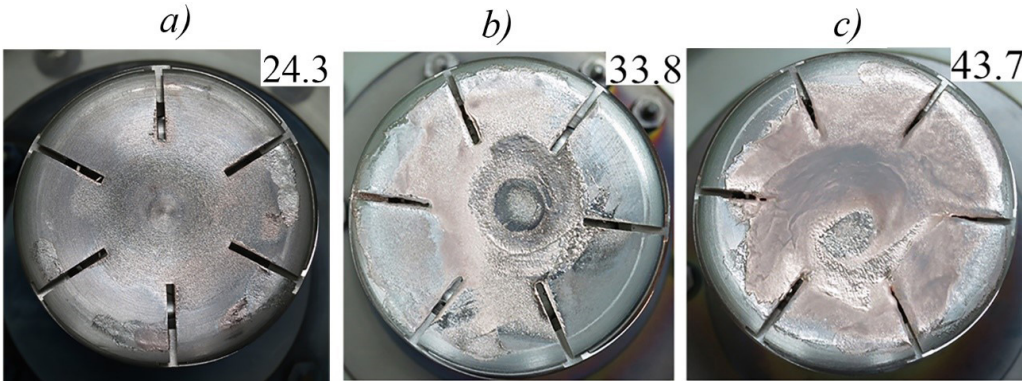

Fig. 6. Photos of anodes after single high-current pulses. The amplitude of the current pulse (kA) is indicated in the upper right corner

parts: radiation in the ultraviolet region ($200 \le \lambda \le 400$) nm and radiation in the visible and infrared regions ($400 \le \lambda \le 1100$) nm. Comparing the measurement results with and without a filter and taking into account the spectral sensitivity of the diode (Fig. 2), we obtain an estimate of the ratio of the power of radiation incident on the diode in the ultraviolet P_{uv} and in the visible and infrared regions of the spectrum P_v. In the arc mode with anodic activity, we obtain $P_{uv}/P_v \approx (5-6) >> 1$. It can be seen that the main part of the power is emitted in the ultraviolet region. This is significant, because in the ultraviolet region ($200 \le \lambda \le 400$) nm, the sensitivity weakly depends on the wavelength and we can determine the radiation power with good accuracy without having information about the spectral distribution of radiation. In the visible and infrared regions, the sensitivity significantly depends on the wavelength and for an accurate assessment, information about the spectral distribution is needed. So far, there is no such information, especially at high currents.

Let us make an estimate of the total radiation power of the discharge P_{uv} in the ultraviolet region, which, as we have seen, differs little from the power in the entire range. To do this, it is necessary to make simplifying assumptions. We will consider the plasma optically thin. Note that both the size of the source (discharge) and the receiver (diode) are much smaller than the distance between them. Note that the radiation comes to the receiver from the entire volume of plasma and falls almost normally. Therefore, we can consider the discharge as a point source, radiating uniformly in all directions. The geometry of the discharge does not matter. If the distance between the source and the receiver would not be so large compared to the size of the source or receiver, then the geometry of the source would play a role. Indeed, radiation from the near–axial region of the source would fall on the diode along the normal, and from the peripheral regions at an acute angle and the law of cosine would work.

If we consider the source to be a point, then under the conditions of this experiment, $4.4 \cdot 10^{-8}$ of the total radiation generated in the discharge falls on the receiver. Figure 7 shows the dependence of the radiation power on the current. These calculations take into account the transparency of the window. It can be seen that in modes with anode activity, the radiation power increases exponentially with an

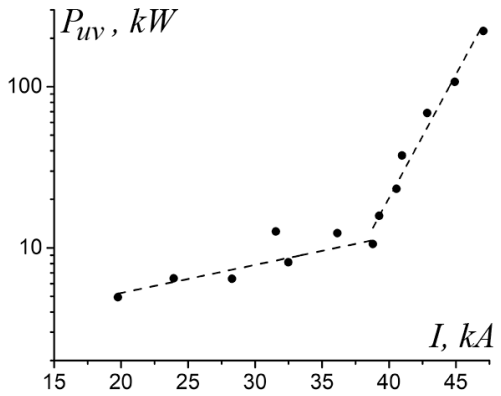

Fig. 7. The maximum radiation power (5.5 ms) in the pulse, depending on the amplitude value of the current

increase in the current amplitude. At a current amplitude of ~ 47 kA, the maximum radiation power (at 5.5 ms) is approximately 14% of the electrical power released at this moment in the discharge. Note that the radiation power in vacuum ultraviolet is not measured by us now. This is planned by us in the future. Taking into account vacuum ultraviolet, the share of radiation power may be significantly higher.

Conclusion

In modes with anode activity, the radiation power increases exponentially with the current. At extremely high currents, when severe erosion occurs, the radiation power can reach almost 15% of the electrical power released in the discharge.

REFERENCES

1. **Raizer Yu.P.,** Fizika gazovogo razryada, Dolgoprudny: Izd. Dom. “Intellekt”, chapter 14. 2009.

2. **Wang L., Jia S., Liu .Y, Chen B., Yang D., and Shi Z.,** Modeling and simulation of anode melting pool flow under the action of high-current vacuum arc, J. Appl. Phys. 107 (11) (2010) Art.no.113306.

3. **Barinov Yu.A., Zabello K.K., Logachev A.A., Poluyanova I.N., Sherstnev E.V., Shkol’nik S.M.,** Radiation Power of a High-Current Vacuum Arc Stabilized by an Axial Magnetic Field in the Visible and UV Ranges of the Spectrum, Tech. Phys. Lett. 47 (2) (2021) 118–121.

4. **Zabello K.K., Poluyanova I.N., Logachev A.A., Begal D.I., Shkol’nik S.M.,** Anode Surface State and Anode Temperature Distribution After Current Zero for Different AMF-Contact Systems IEEE. Plasma Sci. 47 (8) (2019) 3563−3571.

5. **Logachev A.A., Poluyanova I.N., and Klochko S.V.,** Arc voltage as a source of information about arc burning on AMF contacts IEEE Trans. Plas. Sci. 47 (8) (2019) 3572−3578.

6. **Zabello K.K., Poluyanova I.N., Logachev A.A., Barinov A.Yu., Shkol`nik S.M.,** Thermal effect on AMF electrodes at different opening speeds IEEE Trans. Plas. Sci. 49 (4) (2021) 1454−1459.

7. **Barinov Yu.A., Zabello K.K., Logachev A.A., Poluyanova I.N., Sherstnev E.V., Bogdanov A.A., and Shkol'nik S.M.,** Measurements of the radiation power of a high-current vacuum arc at high current densities”, Proc. XXIX ISDEIV (Padova: Italy), 2020, pp. 264–267.

THE AUTHORS

ZABELLO Konstantin K.
zabellok@mail.ioffe.ru
ORCID: 0000-0003-4641-9934

BARINOV Yury A.
yury@mail.ioffe.ru
ORCID: 0000-0002-0329-5743

LOGACHEV Alexander A.
logatchev@mail.ioffe.ru

POLUYANOVA Irina N.
pin@tavrida.com

SHERSTNEV Evgeniy V.
89045512456@ya.ru

SHKOL’NIK Sergey M.
shkolnik@mail.ioffe.ru

Received 25.10.2022. Approved after reviewing 08.11.2022. Accepted 08.11.2022.